


Hypertonicity counteracts MCL-1 and renders BCL-XL a synthetic lethal target in head and neck cancer

Sina Heimer¹, Gertrud Knoll², Patrick Neubert², Karin P. Hammer³, Stefan Wagner³, Richard J. Bauer^{1,4}, Jonathan Jantsch² and Martin Ehrenschwender² 

¹ Department of Oral and Maxillofacial Surgery, University Hospital Regensburg, Regensburg, Germany

² Institute of Clinical Microbiology and Hygiene, University Hospital Regensburg, Regensburg, Germany

³ Department of Internal Medicine II, University Hospital Regensburg, Regensburg, Germany

⁴ Department of Oral and Maxillofacial Surgery, Center for Medical Biotechnology, University Hospital Regensburg, Regensburg, Germany
Open access funding enabled and organized by Projekt DEAL.

Keywords

BCL-XL; head and neck cancer; hyperosmotic stress; MCL-1; NOXA

Correspondence

M. Ehrenschwender, Institute of Clinical Microbiology and Hygiene, University Hospital Regensburg, Franz-Josef-Strauss-Allee 11, Regensburg 93053, Germany
Tel: +49 941 94416440
E-mail: martin.ehrenschwender@ukr.de

(Received 16 December 2019, revised 9 June 2020, accepted 20 July 2020)

doi:10.1111/febs.15492

Head and neck squamous cell carcinoma (HNSCC) is an aggressive and difficult-to-treat cancer entity. Current therapies ultimately aim to activate the mitochondria-controlled (intrinsic) apoptosis pathway, but complex alterations in intracellular signaling cascades and the extracellular microenvironment hamper treatment response. On the one hand, proteins of the BCL-2 family set the threshold for cell death induction and prevent accidental cellular suicide. On the other hand, controlling a cell's readiness to die also determines whether malignant cells are sensitive or resistant to anticancer treatments. Here, we show that HNSCC cells upregulate the proapoptotic BH3-only protein NOXA in response to hyperosmotic stress. Induction of NOXA is sufficient to counteract the antiapoptotic properties of MCL-1 and switches HNSCC cells from dual BCL-XL/MCL-1 protection to exclusive BCL-XL addiction. Hypertonicity-induced functional loss of MCL-1 renders BCL-XL a synthetically lethal target in HNSCC, and inhibition of BCL-XL efficiently kills HNSCC cells that poorly respond to conventional therapies. We identify hypertonicity-induced upregulation of NOXA as link between osmotic pressure in the tumor environment and mitochondrial priming, which could perspective be exploited to boost efficacy of anticancer drugs.

Introduction

Head and neck squamous cell carcinomas (HNSCCs) are among the most common malignancies worldwide [1]. Research efforts during the last decades increased the understanding of this disease but failed to bring up clinically meaningful discoveries. Currently available treatments include surgical eradication, radiotherapy, and chemotherapy but are often ineffective [2]. The mitochondria-controlled (intrinsic) apoptotic pathway largely determines sensitivity or resistance to anti-cancer treatments [3]. Intrinsic apoptosis proceeds by

insertion of the pore-forming proteins BAX and/or BAK in the outer mitochondrial membrane (OMM). Subsequent release of apoptosis-promoting molecules from the mitochondrial intermembrane space allows formation of the apoptosome, a scaffold that facilitates activation of caspase-9 and (further downstream) activation of caspase-3 and caspase-7, the executioners of apoptosis [4]. To prevent accidental cell death induction, a sophisticated network of pro- and antiapoptotic BCL-2 family proteins imposes a threshold (also

Abbreviations

CI, combination index; EGFR, epidermal growth factor receptor; ER, endoplasmic reticulum; HNSCC, head and neck squamous cell carcinoma; OMM, outer mitochondrial membrane.

referred to as ‘mitochondrial priming’) that apoptosis-promoting stimuli must meet for BAX/BAK activation [5]. In cancer cells, mitochondrial priming directly correlates with response to chemotherapy [6]. Consequently, modulating mitochondrial priming by targeting the safeguards of the OMM (e.g., BCL-2, BCL-XL, and MCL-1) emerged as a novel therapeutic approach [7]. Small molecules that occupy the BH3 domain-binding groove (‘BH3 mimetics’) of antiapoptotic BCL-2 family proteins (e.g., ABT-199 targeting BCL-2, WEHI-539 targeting BCL-XL, or S63845 targeting MCL-1) abrogate their protective function and prime mitochondria for death [8–10]. Synergistic effects of BH3 mimetics with other treatment modalities have been reported in HNSCC [11,12], but thus far failed to demonstrate efficacy in clinical trials [13]. This is not surprising, as most cancer cells rely at least on two antiapoptotic BCL-2 family proteins (e.g., BCL-XL and MCL-1) to ensure OMM integrity [14]. Antiapoptotic BCL-2 family proteins exhibit functional redundancy and can play compensatory roles, which allows most cancer cells to survive selective inhibition of only one of their mitochondrial safeguards.

Head and neck squamous cell carcinoma often face harsh environmental conditions such as hypoxia and mechanical stress [15]. Adaption to these challenges involves cellular stress responses that ensure survival but can concomitantly alter the cell’s apoptotic threshold [16]. For example, accommodation to hyperosmotic stress in the tumor environment also affects levels of BCL-2 family proteins [17]. Hyperosmotic stress (or hypertonicity) occurs when osmolytes that cannot passively diffuse across the plasma membrane (such as NaCl or trehalose) establish an osmotic pressure gradient between the intra- and extracellular space. Hypertonicity triggers an adaptive cellular response to compensate for environmental changes, maintain cellular homeostasis, and ensure survival [18]. When osmoadaptive mechanisms fail or hypertonicity persists, a variety of perturbing effects such as cell cycle arrest, DNA damage, inhibition of transcription/translation, mitochondrial depolarization, and apoptosis induction can occur [19]. Notably, hypertonicity-induced apoptosis is controlled by the mitochondria and regulated by BCL-2 family proteins [20].

In this study, we show that the response of HNSCC cells to hypertonic conditions in the tumor environment transforms dual BCL-XL/MCL-1 dependency into exclusive BCL-XL addiction. Hypertonicity-induced upregulation of the proapoptotic BH3-only protein NOXA counteracts the antiapoptotic function of MCL-1 and shifts maintenance of OMM integrity from a cooperative BCL-XL/MCL-1 interplay to

exclusive BCL-XL dependency. Inhibition of BCL-XL under hypertonic conditions is synthetically lethal and efficiently kills cancer cells that poorly respond to epidermal growth factor receptor (EGFR) inhibition or radiotherapy. Our results characterize hypertonicity-induced upregulation of NOXA as molecular link between osmotic pressure in the tumor environment and mitochondrial priming in HNSCC. Functionally, we show that an adaptive cellular response to changing conditions in the tumor microenvironment can be utilized to sensitize HNSCC cells to apoptosis. Our findings could be exploitable in future treatment strategies to boost efficacy of anticancer drugs.

Results

Hypertonicity counteracts MCL-1 in HNSCC cells

Previous reports highlighted a key role for both BCL-XL and MCL-1 in HNSCC survival [10,21]. Accordingly, the BCL-XL-specific inhibitor WEHI-539 showed little cytotoxicity (Fig. 1A) in various HNSCC cell lines as a single agent, but synergized with the MCL-1-targeting compound S63845 in cell death induction (Fig. 1A and Table 1). In line with dual BCL-XL/MCL-1 dependency, simultaneous knock-down of BCL-XL and MCL-1 displayed cytotoxic effects (Fig. 1B). In HNSCC cell lines exposed to a hypertonic environment, however, exclusive inhibition of BCL-XL was sufficient to trigger cell death, even in the absence of a pharmacological MCL-1 inhibitor (Figs 1C,D,F,H,I and 2B). Calculation of the combination index (CI) confirmed synergistic cell death induction by WEHI-539 and NaCl (Table 1). WEHI-539-induced loss of viability under hyperosmotic stress showed hallmarks of apoptotic cell death such as increased activity of the effector caspases-3/7 (Fig. 1E, G) and annexin-V/7-AAD positivity (Fig. 2C). Down-regulation of BAX, the main effector protein of the intrinsic apoptosis pathway, or addition of the pan-caspase inhibitor QVD-OPh expectedly reduced cytotoxicity of WEHI-539 under hypertonic conditions (Fig. 2A,D). Hyperosmotic stress also enhanced sensitivity of HNSCC spheroid cell cultures for BCL-XL inhibition (Fig. 3A,B). Besides WEHI-539, other BCL-XL targeting agents such as ABT-737 (targeting BCL-XL, BCL-2, and BCL-W) efficiently triggered cell death under hypertonic conditions (Fig. 3C,D,E,G). Selective inhibition of BCL-2 (using ABT-199) did not cooperate with hypertonicity in cell death induction (Fig. 3F), suggesting that indeed ABT-737-mediated BCL-XL inhibition is critical. Accordingly, cytotoxicity of the MCL-1 inhibitor S63845 was not enhanced

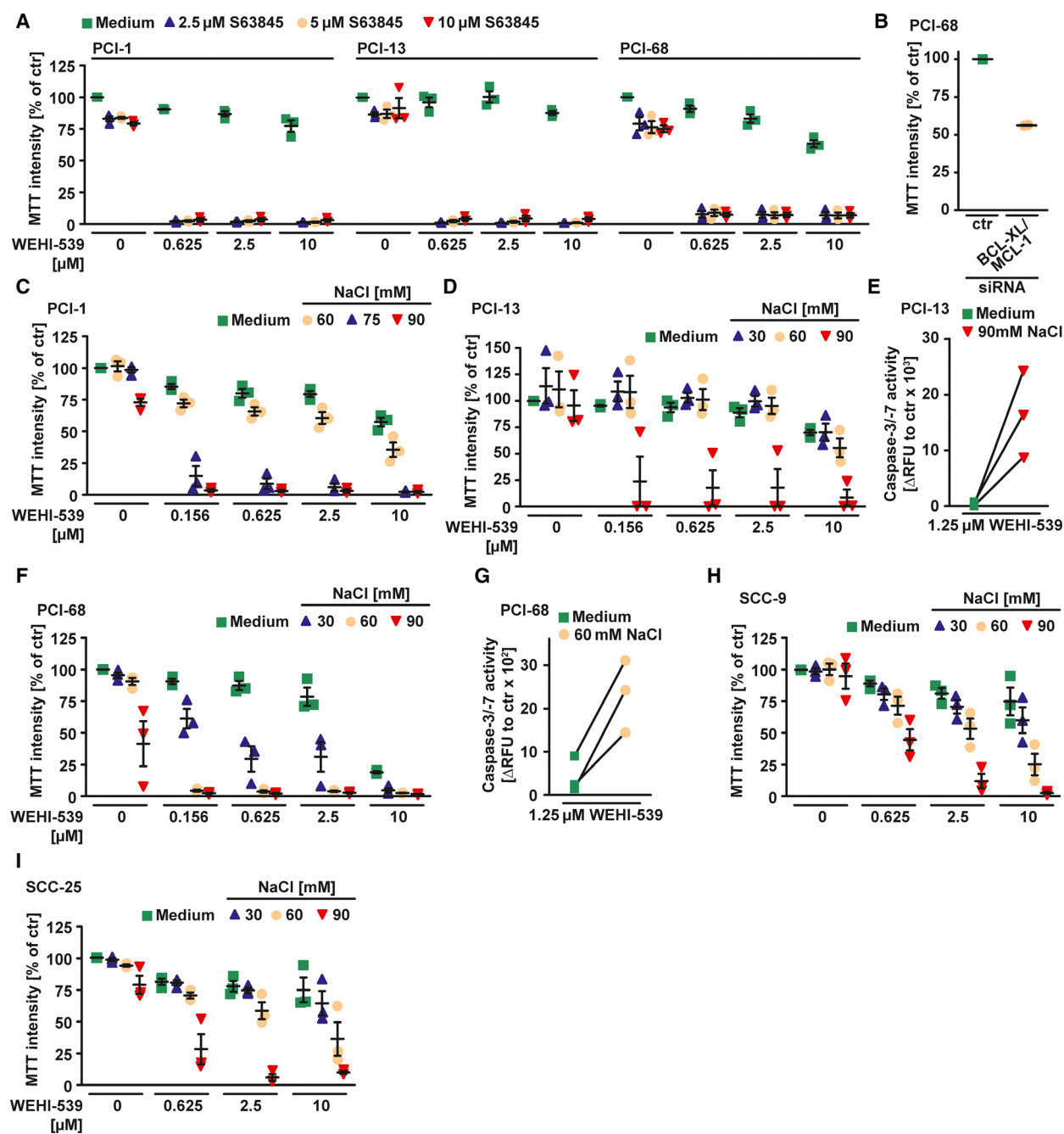


Fig. 1. Hyperosmotic stress shifts BCL-XL/MCL-1-protected HNSCC cells to exclusive BCL-XL addiction. (A) Cells were challenged with the indicated concentrations of the BCL-XL inhibitor WEHI-539 in the presence and absence of the MCL-1 inhibitor S63845. (B) Cells were transfected with siRNA oligonucleotides targeting BCL-XL and MCL-1 or nontargeting control (ctr). After 24 h, cells treated with control siRNA were challenged with WEHI-539 (1.25 μ M) in the presence and absence of S63845 (1.25 μ M) for another 18 h. (C, D, F, H, I) Cells were challenged with the indicated concentrations of the BCL-XL inhibitor WEHI-539 in the presence and absence of NaCl. (E, G) Cells were challenged with WEHI-539 (1.25 μ M) in the presence and absence of the indicated concentrations of NaCl for 18 h. Caspase-3/7 activity was assessed using the fluorogenic substrate (DEVD)₂-R110. For (A, C, D, F, H, I), data points and mean \pm SEM from three independent experiments are shown; for (B), data points and mean from two independent experiments are shown; for (E, G), individual data points of at least two independent experiments are shown. RFU, relative fluorescence units.

Table 1. Combination index of BCL-XL-targeting BH3 mimetics in the presence of MCL-1 inhibitors or hyperosmotic stress. Synergistic effects on WEHI-539-mediated cell death by combinatorial treatment with the MCL-1-selective inhibitor S63845 (2.5 μ M) and NaCl-induced hypertonicity (PCI-1: 75 mM NaCl, PCI-13: 90 mM NaCl, PCI-68: 60 mM NaCl). Synergism in terms of cell death induction was quantitatively assessed by calculating the CI from mean values from three independent experiments. CI values < 1 are considered synergistic, and CI values > 1 indicate antagonistic effects.

	S63845	NaCl
PCI-1		
WEHI-539 (μ M)		
0.625	2.20E-4	4.92E-3
2.5	4.02E-4	1.14E-2
10	1.13E-3	1.10E-2
PCI-13		
WEHI-539 (μ M)		
0.625	4.25E-5	3.46E-3
2.5	4.25E-5	1.38E-2
10	4.25E-5	1.93E-2
PCI-68		
WEHI-539 (μ M)		
0.625	6.28E-3	6.11E-3
2.5	1.09E-2	2.28E-2
10	3.41E-2	6.46E-2

under hyperosmotic stress (Fig. 3F). In sum, our data suggested that hyperosmotic stress shifted combined BCL-XL/MCL-1 dependency of HNSCC cells to exclusive BCL-XL addiction by selectively counteracting the antiapoptotic function of MCL-1.

Hypertonicity-induced NOXA upregulation shifts dual BCL-XL/MCL-1 dependency toward exclusive BCL-XL addiction

The hypertonicity-induced loss of MCL-1 protection and the resulting switch from combined BCL-XL/MCL-1 to exclusive BCL-XL dependency were related neither to reduction of intracellular BCL-XL/MCL-1 levels nor to reduced expression of the corresponding genes (Fig. 4A,B). Notably, interaction with BH3-only proteins such as NOXA can modulate the antiapoptotic function of MCL-1 [5]. Indeed, hypertonicity changed cellular NOXA levels. NOXA was barely detectable under isotonic conditions but increased transiently upon hyperosmotic stress (Fig. 4A,C). Other apoptosis-promoting BCL-2 family proteins, however, displayed no hypertonicity-induced upregulation (Fig. 4A). Downregulation of NOXA was sufficient to rescue HNSCC cells challenged with the BCL-XL inhibitor WEHI-539 under hypertonic conditions,

whereas knockdown of BIM had no effect (Fig. 4D). This indicated functional relevance for hypertonicity-induced NOXA upregulation to shift combined BCL-XL/MCL-1 toward exclusive BCL-XL dependency.

Hypertonicity triggers Ca^{2+} release from the ER in the absence of ER stress and limits cancer cell proliferation

Hypertonicity is a known trigger of ER stress [22]. This adaptive response to cell-intrinsic and cell-extrinsic stress has been linked to tumorigenic effects [23], but also to cancer cell killing via Ca^{2+} -dependent NOXA upregulation [24]. Indeed, hyperosmotic stress promoted a rise in cytoplasmic Ca^{2+} (Fig. 5A). Hypertonicity also increased cytoplasmic Ca^{2+} levels in cells cultured in a Ca^{2+} -free Tyrode's salt solution and was not affected by coincubation with the BCL-XL inhibitor WEHI-539 (Fig. 5B). Apparently, hypertonicity triggered release of Ca^{2+} from intracellular stores such as the ER. Calcium release from this organelle is, among other mechanisms, controlled by ryanodine receptors [25]. Pharmacological inhibition of ryanodine receptors and the selective Ca^{2+} chelator BAPTA-AM attenuated the hypertonicity-induced rise in intracellular Ca^{2+} (Fig. 5C). Cyclosporine A, an inhibitor of mitochondrial Ca^{2+} release, was not effective (Fig. 5D), which strengthened a role for the ER in boosting intracellular Ca^{2+} levels during hyperosmotic stress. However, we were not able to detect markers of ER stress (such as ATF-4 and ATF-6) in cells challenged with 60 mM NaCl (Fig. 5E). BAPTA-AM and ryanodine receptor antagonists even aggravated cytotoxicity of NaCl/WEHI-539 treatment (Fig. 5F,G). Elevated intracellular Ca^{2+} levels can also activate p53, a key transcription factor for NOXA [26,27]. Knockdown of p53, however, did not protect PCI-68 cells from NaCl/WEHI-539-induced cell death (Fig. 5H). Collectively, these data did not indicate critical involvement of elevated cytoplasmic Ca^{2+} levels, ER stress, and p53 in disruption of antiapoptotic MCL-1 activity and the resulting exclusive BCL-XL addiction.

Notably, Na^+ influx and osmotic stress have previously been linked to enhanced migration and proliferation of cancer cells [28–30]. Indeed, NaCl supplementation of the cell culture media increased intracellular Na^+ levels in HNSCC cells in a dose-dependent manner (Fig. 6A). Combinatorial treatment with WEHI-539/NaCl resulted in more pronounced cytoplasmic Na^+ accumulation, while WEHI-539 alone had no effect (Fig. 6B). However, proliferation and migration of HNSCC cells cultured under hyperosmotic conditions were even reduced (Figs 6C and 7A,

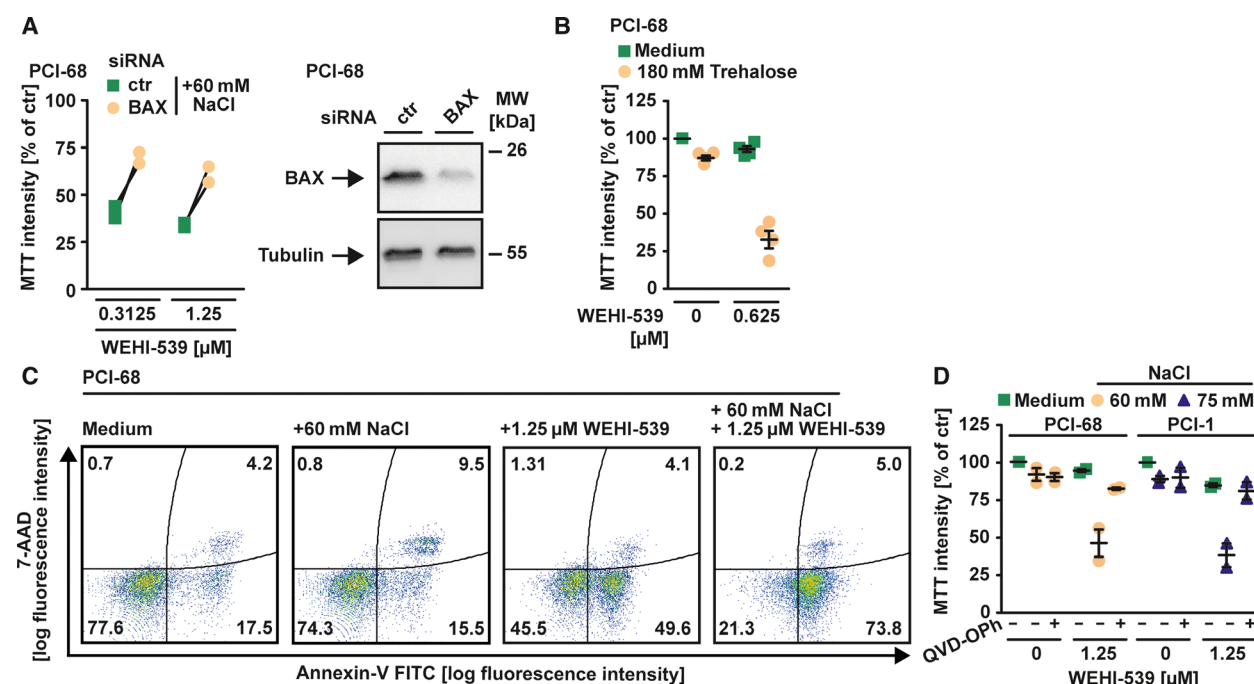


Fig. 2. BCL-XL inhibition under hyperosmotic conditions triggers apoptosis. (A) PCI-68 cells were transfected with siRNA oligonucleotides targeting BAX or nontargeting control. After 48 h, cells were challenged with the indicated concentration of WEHI-539 presence and absence of NaCl for another 18 h. (B) Cells were challenged with WEHI-539 (0.625 μM) in the presence and absence of trehalose (180 mM) for 18 h. (C) PCI-68 cells were treated with WEHI-539 (1.25 μM) in the presence and absence of NaCl (60 mM). After 8 h, cells were analyzed by flow cytometry for 7-AAD- and annexin-V positivity. (D) Cells were challenged with the indicated concentrations of WEHI-539 in the presence and absence of NaCl and/or QVD-OPh (50 μM). For (A), individual data points of two independent experiments are shown; for (B and D), data points and mean ± SEM from three independent experiments are shown; for (C), data shown are representative of two experiments performed. RFU, relative fluorescence units.

B). Hyperosmotic stress also efficiently boosted cytotoxicity of BCL-XL inhibition under low oxygen conditions (Fig. 6D,E), which are commonly encountered in HNSCC and associated with poor treatment response [31]. Thus, hypertonic conditions did not enhance proliferation of HNSCC cells but efficiently inhibited MCL-1 even in a hypoxic tumor environment.

BCL-XL inhibition under hyperosmotic stress efficiently kills HNSCC cells that poorly respond to EGFR inhibition or radiotherapy

Treatment options for HNSCC are scarce. Inhibitors of EGFR occupy the tyrosine kinase domain and are the only approved targeted drugs, but often display limited efficacy. Accordingly, erlotinib killed only up to ~50% of cells in the HNSCC cell lines tested (Fig. 8A–F). With the notable exception of PCI-1 cells, hyperosmotic stress did expectedly not aggravate cytotoxicity of erlotinib. In contrast, counteracting MCL-1 (either through pharmacological inhibition or

by establishing hypertonic conditions) enabled a full-blown killing of all cell lines upon treatment with the BCL-XL inhibitor WEHI-539 (Fig. 1C,D,F,H,I).

In HNSCC treatment, radiotherapy is still the mainstay and resistance is a major cause of poor survival rates [2]. Exposure to high radiation doses (12 Gy) killed only a fraction of HNSCC cells within 72 h, irrespective whether cells were cultured under iso- or hypertonic conditions (Fig. 8G–I). Targeting BCL-XL under hypertonic conditions, however, was sufficient for near-complete cancer cell elimination within 24 h even in the absence of radiation. These data recapitulated the limitations of currently available HNSCC treatments and indicated that approaches targeting antiapoptotic BCL-2 family members could complement existing therapies.

Discussion

Our study highlights that hyperosmotic stress in the tumor environment (a) shifts dual BCL-XL/MCL-1 dependency of HNSCC cells to exclusive BCL-XL

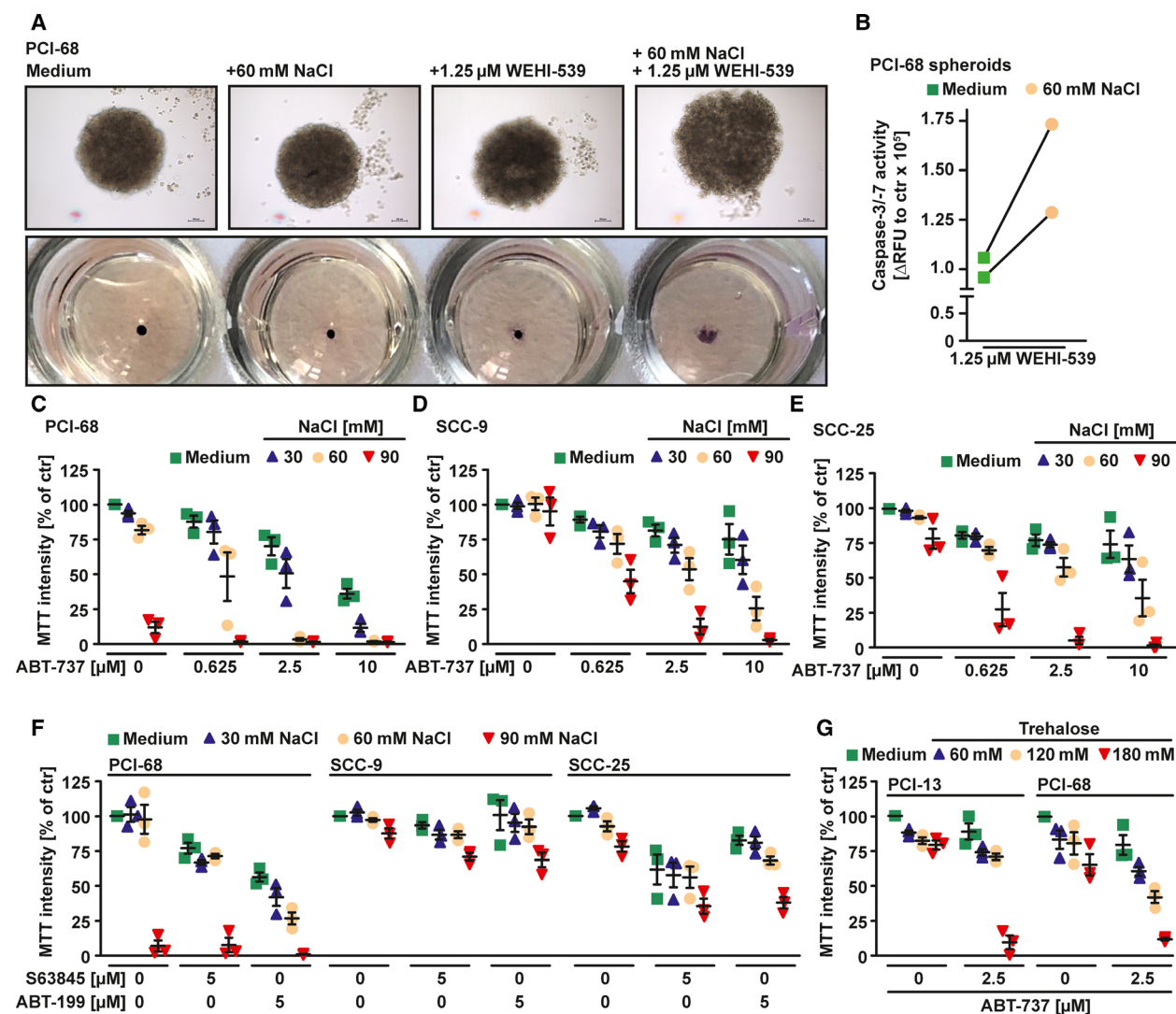
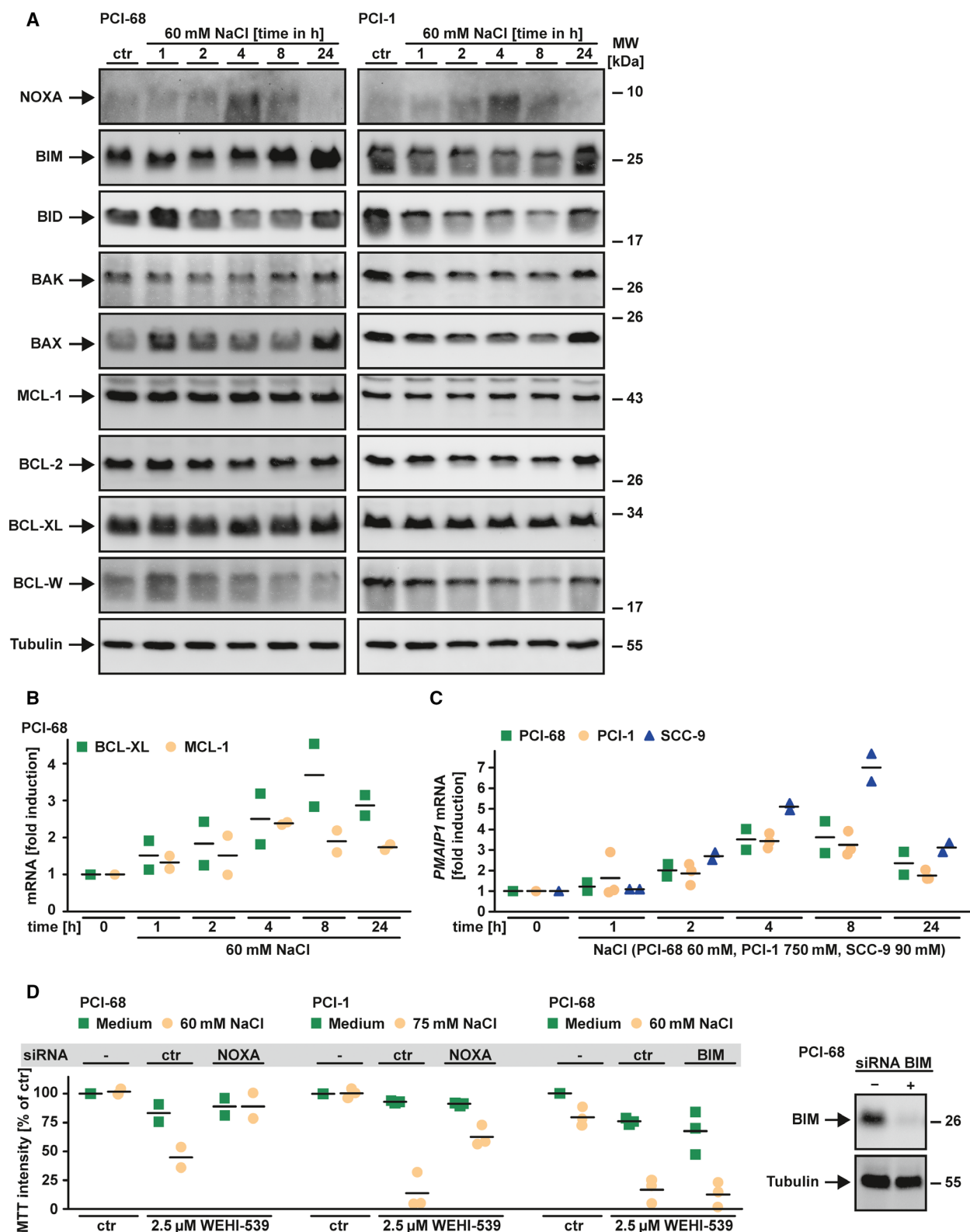


Fig. 3. Hypertonicity counteracts the antiapoptotic function of MCL-1. (A) Spheroids of PCI-68 cells were treated with WEHI-539 (1.25 μ M) in the presence and absence of NaCl (60 mM). Upper panel: changes in spheroid morphology upon NaCl/WEHI-539 treatment. Scale bar: 100 μ m. Lower panel: Cells were treated as above, but MTT staining was used to determine cell viability. (B) Spheroid cultures of PCI-68 cells were challenged with WEHI-539 (1.25 μ M) in the presence and absence of NaCl (60 mM) for 18 h. Caspase-3/-7 activity was assessed using the fluorogenic substrate (DEVD)₂-R110. (C–G) Cells were challenged with the indicated concentrations of ABT-737, ABT-199, and S63845 in the presence and absence of the indicated concentrations of the osmotically active solutes NaCl (C–F) or trehalose (G). For (A), data shown are representative of two experiments performed; for (B), individual data points of two independent experiments are shown; for (C–G), data points and mean \pm SEM from three independent experiments are shown. RFU, relative fluorescence units.

Fig. 4. NOXA upregulation is essential for hypertonicity-enforced BCL-XL addiction. (A) Cells were challenged with NaCl (PCI-68: 60 mM, PCI-1: 75 mM) for the indicated periods. After washing and lysis, western blot analysis was performed with antibodies specific for the indicated proteins. (B) PCI-68 cells were challenged with NaCl (60 mM) for the indicated periods. mRNA levels of genes encoding BCL-XL and MCL-1 were analyzed by qPCR. (C) Cells were challenged with the indicated concentrations of NaCl for the indicated periods. mRNA levels of *PMAIP1* (encoding NOXA) were analyzed by qPCR. (D) Left panel: Cells were transfected with siRNA oligonucleotides targeting NOXA or BIM or nontargeting control. After 48 h, cells were treated with WEHI-539 (2.5 μ M) in the presence and absence of the indicated concentrations of NaCl for another 18 h. Right panel: Western blot analysis using specific antibodies for the indicated proteins assessed knockdown efficacy. For (A), data shown are representative of two experiments performed. For (B–D), data points and mean from at least two independent experiments are shown.



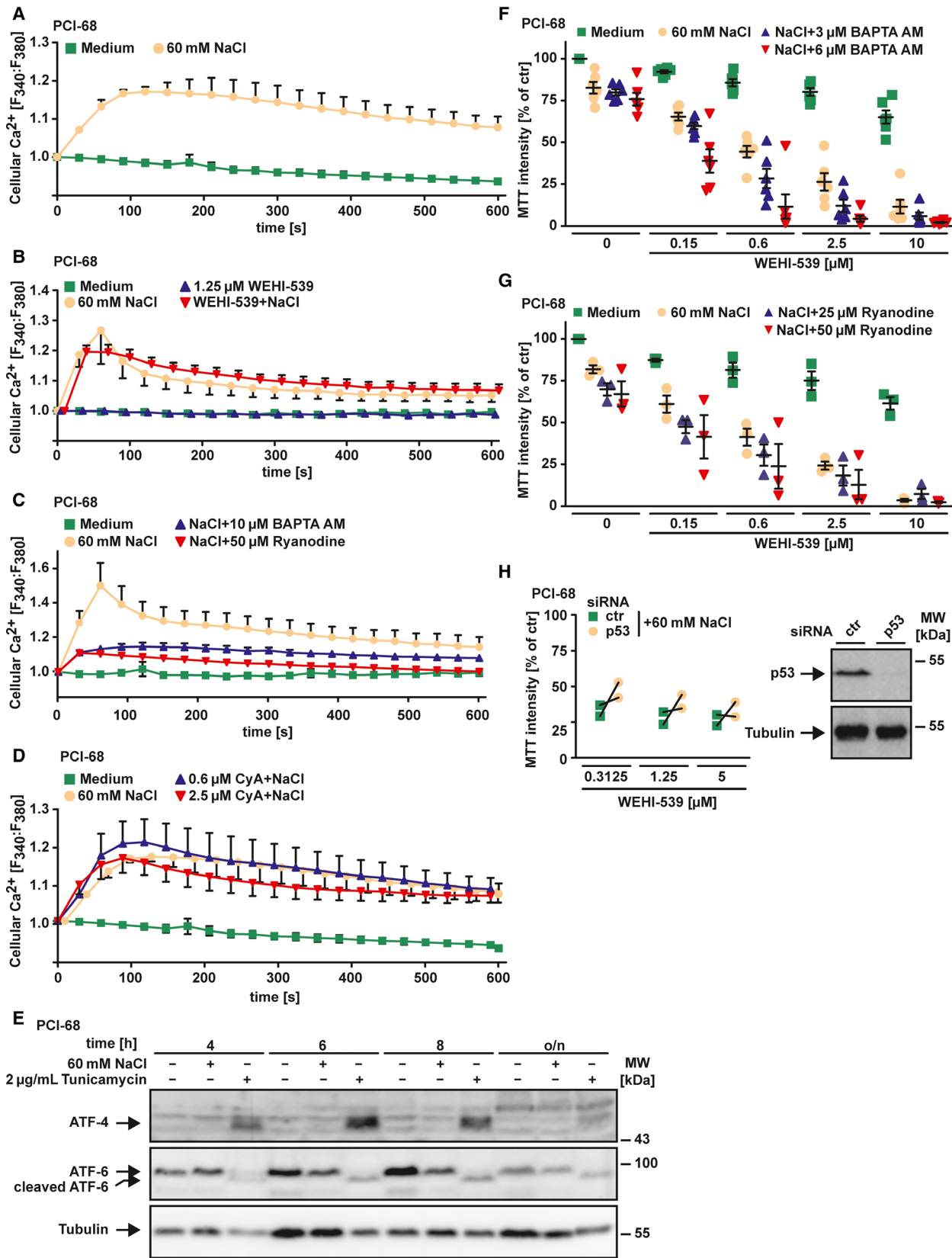


Fig. 5. Transition to exclusive BCL-XL dependency is not a consequence of ER stress or cytoplasmic Ca^{2+} increase. (A) PCI-68 cells were challenged with NaCl (60 mM). Intracellular calcium levels were measured using the ratiometric Ca^{2+} indicator Fura-2 in a Ca^{2+} -containing Tyrode's solution. (B) PCI-68 cells were challenged with WEHI-539 (1.25 μM) in the presence and absence of NaCl (60 mM). Intracellular calcium levels were measured as above, but in a Ca^{2+} -free Tyrode's solution. (C) Cells were treated with NaCl (60 mM) in the presence and absence of the Ca^{2+} chelating agent BAPTA-AM and the ryanodine receptor antagonist ryanodine. Intracellular calcium levels were measured as above in a Ca^{2+} -free Tyrode's solution. (D) PCI-68 cells were challenged with NaCl (60 mM) in the presence of cyclosporine A (0.6 and 2.5 mM), which inhibits calcium release from the mitochondria via the permeability transition pore. Intracellular calcium levels were measured using the ratiometric Ca^{2+} indicator Fura-2. (E) Cells were treated for the indicated periods with NaCl (60 mM) or the ER stress-inducing inhibitor tunicamycin (2 $\mu\text{g}\cdot\text{mL}^{-1}$). After washing and lysis, western blot analysis was performed with antibodies specific for the indicated proteins. (F, G) Cells were challenged with the indicated concentrations of WEHI-539 in the presence and absence of BAPTA-AM and ryanodine for 18 h. (H) PCI-68 cells were transfected with siRNA oligonucleotides targeting p53 or nontargeting control. After 48 h, cells were challenged with the indicated concentration of WEHI-539 in the presence and absence of NaCl for another 18 h. For (A–D and F–H), shown are data points and mean \pm SEM from two or three independent experiments; for (E), data shown are representative of two experiments performed. CyA, cyclosporine A.

addiction in a NOXA-dependent manner; (b) does not promote ER stress, cancer growth, or migration; and (c) grants contextual synthetic lethality to BCL-XL inhibitors. The biophysical properties in the microenvironment of solid tumors (such as oxygen level, interstitial fluid pressure, and pH) differ greatly from healthy tissues and impair treatment response [32]. On the contrary, components of the tumor environment itself emerged as therapeutic targets in HNSCC [33]. The tumor microenvironment also requires proactive adaptation of cancer cells to ensure survival. Targeting processes or consequences of this environment-imposed cellular response are often detrimental and summarized in the concept of contextual synthetic lethality [34].

With this study, we took this approach a step further. Artificial manipulation of the osmotic pressure in the tumor environment enforces an adaptive cellular response that ‘accidentally’ compromises the cell’s antiapoptotic safeguard mechanism. The readiness to undergo apoptotic cell death consequently increases: HNSCC cells are primed for death. Apparently, lowering the threshold for cell death induction and exclusive BCL-XL addiction involves hypertonicity-induced upregulation of NOXA (Fig. 4C,D). This is in line with previous studies that reported a decisive role for NOXA in apoptosis induction upon inhibition of BCL-2 family proteins [11,12,35–37]. Although a Ca^{2+} -dependent mechanism of NOXA upregulation has been described [24], our findings suggest a protective rather than a cell death promoting role for the hypertonicity-induced rise in cytoplasmic Ca^{2+} (Fig. 5F). The intracellular calcium response to hyperosmotic stress is well established in a variety of cell types, including cancer cells [38,39]. Calcium signaling in hypertonic environments can promote both osmoadaptive processes and apoptosis [40–42]. In cancer cells, elevated intracellular Ca^{2+} levels boost efficacy of anticancer drugs [43]. In our experimental setup, however,

Ca^{2+} -induced survival pathways seem to be dominant (Fig. 5F).

Our study demonstrates that osmotic pressure (and potentially other biophysical factors) in the tumor microenvironment can change dependencies of cancer cells on antiapoptotic BCL-2 family proteins and therefore modulate the apoptotic threshold. These environment-related changes in mitochondrial priming should be taken into account when predicting sensitivity of cancer cells toward inhibitors of BCL-2 family proteins. Solid tumors, for example, often exhibit elevated pressure in the tumor bulk due to fluid pressure and solid stress [44]. Mapping dependencies on BCL-2 family proteins under standardized, nonphysiological conditions *in vitro* might therefore inaccurately predict susceptibilities/resistances *in vivo*. Exploring the interdependency of biophysical factors in the tumor environment and death priming of cancer cells could also lay open previously unrecognized therapeutic targets. Regardless of any properties of the tumor environment, it is important to note that an intact intrinsic apoptosis pathway remains essential for efficient cancer cell killing with BH3 mimetics.

The cellular response to hyperosmotic stress is complex and profoundly alters a cell’s state [19]. Immediate effects occur within minutes and include osmotic efflux of water, cell shrinkage, increased intracellular ionic strength, DNA double-strand breaks, cytoskeletal rearrangements, and elevated levels of reactive oxygen species [45–47]. During the process of adaption (lasting hours to days), preexisting ion transport systems increase intracellular concentrations of potassium, sodium, and chloride ions, which ultimately causes water influx and a regulatory volume increase [48]. Multiple pathways signal activation of the transcription factor nuclear factor of activated T-cell 5 (NFAT5) and ensure increased expression/activity of stress proteins such as p53 and heat-shock proteins [49–51]. A cell accommodated to hypertonic stress

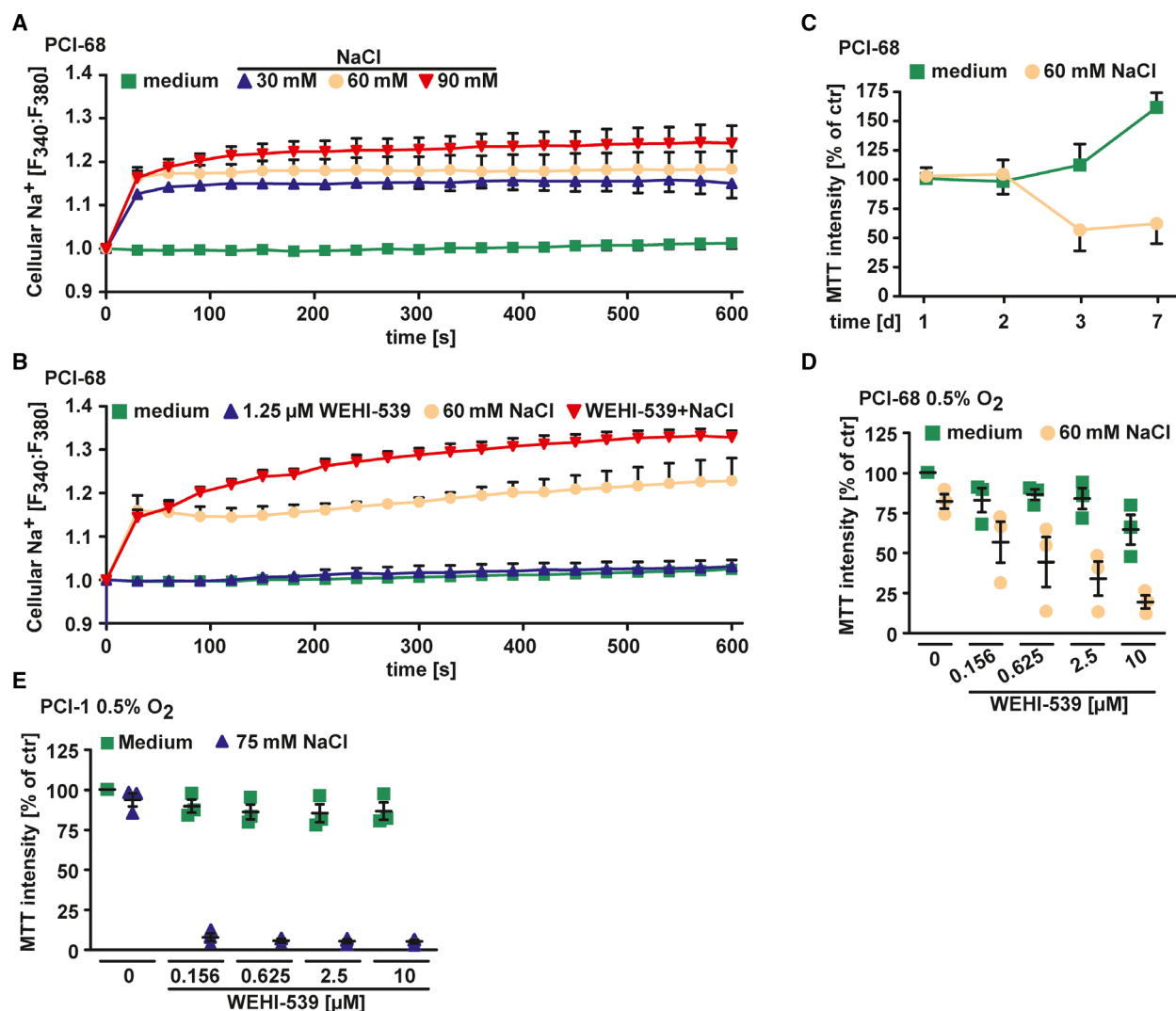


Fig. 6. Hyperosmotic stress reduces proliferation of HNSCC cells and boosts WEHI-539 cytotoxicity in a hypoxic environment. (A, B) PCI-68 cells were challenged with the indicated concentrations of NaCl in the presence and absence of WEHI-539 (1.25 μ M). Intracellular sodium levels were measured using the ratiometric Na^+ indicator SBFI. (C) PCI-68 cells were incubated with NaCl (60 mM) for the indicated periods. Cell proliferation was determined by MTT staining. (D, E) Cells were cultured under low oxygen conditions (0.5%) and challenged with the indicated concentrations of WEHI-539 in the presence and absence of NaCl (60 mM) for 18 h. For (A, B, D, E), data points and mean \pm SEM from three independent experiments are shown; for (C), mean \pm SEM from three independent experiments is shown.

displays normal cell volume, ionic strength, cell cycle, and transcription/translation. Nevertheless, initial perturbations such as DNA damage and increased protein oxidation persist [19]. Even after adaption, the state of a hypertonicity-exposed cell remains strikingly different from isotonic conditions. Notably, no specific osmosensor has been identified in mammalian cells thus far. Instead, all of the above-mentioned immediate effects of hypertonicity can signal an osmoregulatory response [19]. Earlier studies already indicated that adaption to hypertonic conditions can alter the

apoptotic threshold of cells. Hyperosmotic stress can repress translation of MCL-1 [52]. This could account for the functional loss of MCL-1 in HNSCC cells under hypertonic conditions (Fig. 1C,D,F,H,I) despite upregulation of MCL-1 mRNA (Fig. 4B). Facilitating the activation of the mitochondria-controlled apoptosis pathway also sensitized cancer cells to death receptor-induced apoptosis [53,54]. Our current study highlights hypertonicity-induced upregulation of NOXA as molecular link between osmotic pressure in the tumor environment and mitochondrial priming in HNSCC.

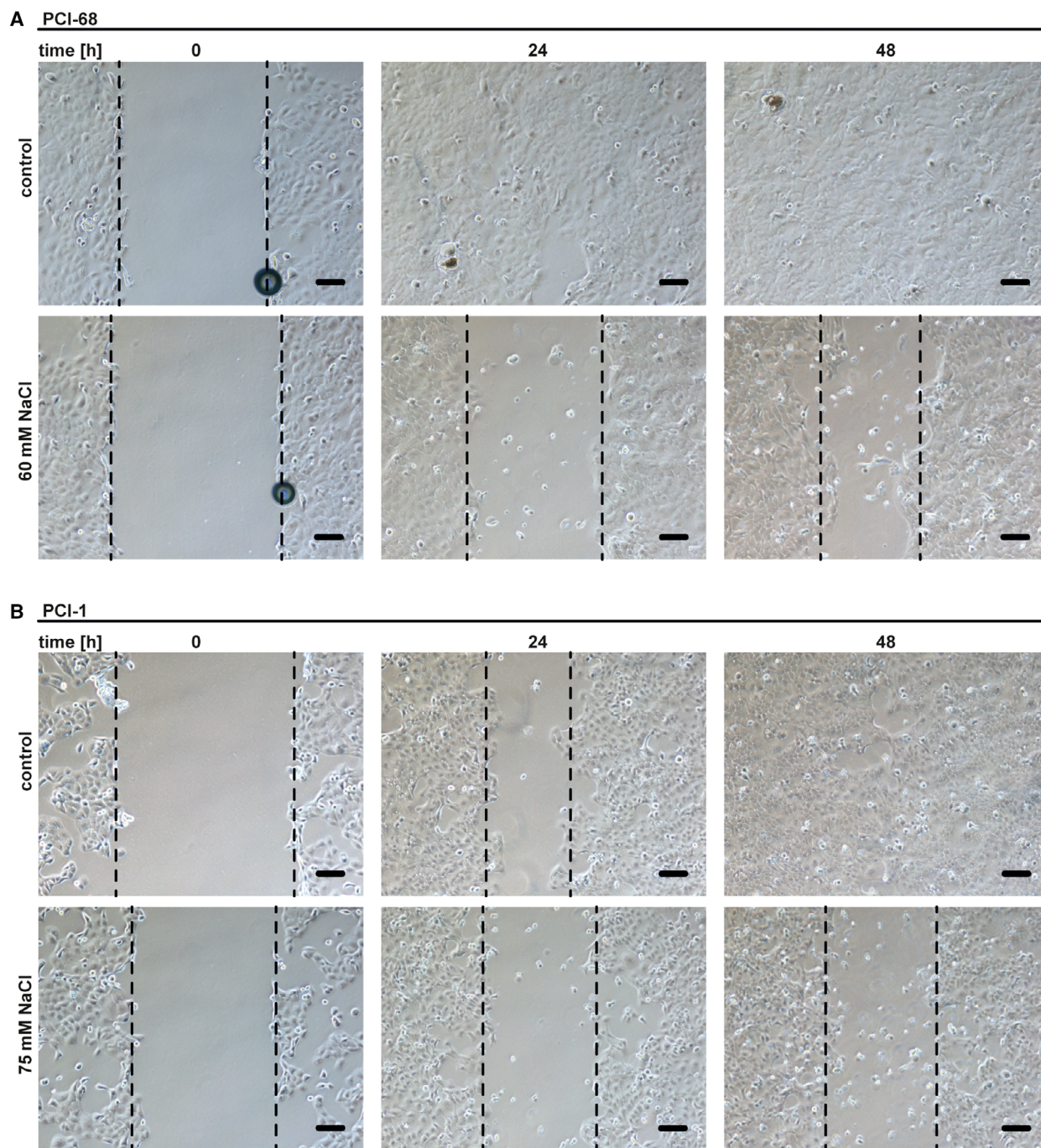


Fig. 7. Migration of HNSCC cells is reduced under hypertonic conditions. (A, B) Wound healing assays of PCI-68 and PCI-1 cells in the presence and absence of NaCl. Phase-contrast images were taken after 0, 24, and 48 h. Scale bar = 50 μ m. The dashed lines indicate the growth front. For (A and B), data shown are representative of two experiments performed.

Nevertheless, the critically involved signaling pathways and/or osmoadaptive processes remain enigmatic.

We are aware that the complexity to establish hypertonic conditions in the tumor environment may be a

limiting factor for therapeutic exploitation of our findings. However, in solid tumors that are easily reachable, direct delivery of osmotically active solutes or continuous release from implantable devices could be

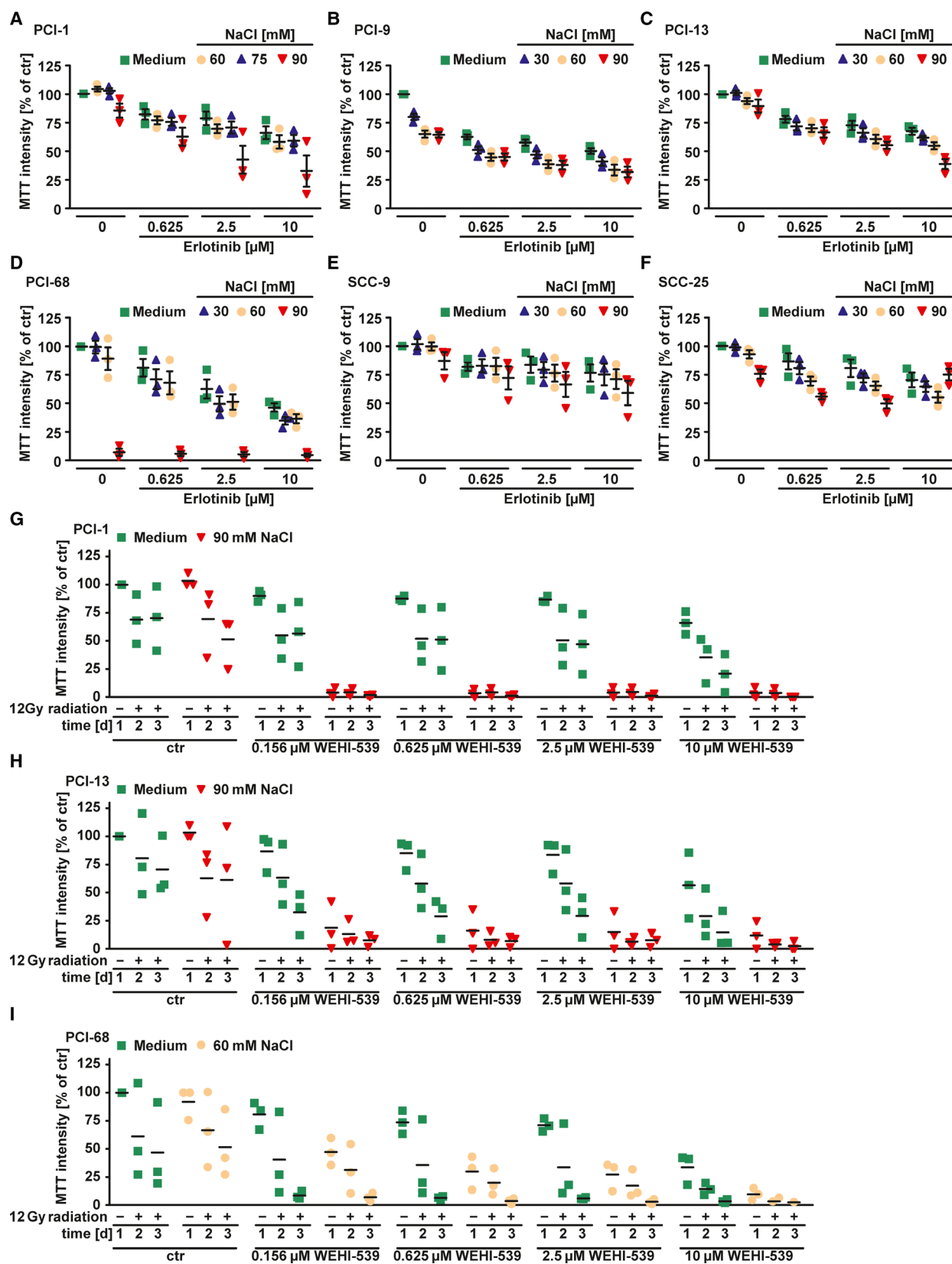


Fig. 8. Targeting BCL-XL under hyperosmotic stress efficiently eliminates HNSCC cells that poorly respond to radiotherapy or EGFR inhibition. (A–F) Cells were challenged with the EGFR inhibitor erlotinib in the presence and absence of the indicated concentrations of NaCl for 18 h. (G–I) Cells were treated with the indicated concentrations of WEHI-539 in the presence and absence of NaCl (60 or 90 mM) and/or irradiated as indicated (12 Gy). Cell viability was assessed at days 1, 2, and 3 using MTT staining. For (A–F), data points and mean \pm SEM from three independent experiments are shown; for (G–I), data points and mean from three independent experiments are shown.

feasible and boost efficacy of our scarce armamentarium currently available for HNSCC treatment.

Materials and methods

Cell lines, antibodies, and reagents

SCC-9 and SCC-25 cells were obtained from LGC Standards GmbH (Wesel, Germany). PCI-1, PCI-13, and PCI-68 have been described previously [55]. PCI-1, PCI-13, and PCI-68 cells were maintained in RPMI 1640 medium (PAN-Biotech, Aidenbach, Germany) with 10% (v/v) fetal bovine serum (Sigma, Steinheim, Germany). SCC-9 and SCC-25 cells were grown in a 1 : 1 mixture of Dulbecco's modified Eagle's medium (DMEM) and Ham's F12 medium containing 1.2 g·L⁻¹ sodium bicarbonate, 2.5 mM L-glutamine, 15 mM HEPES, and 0.5 mM sodium pyruvate (Thermo Fisher, Waltham, MA, USA) supplemented with 400 ng·mL⁻¹ hydrocortisone and 10% (v/v) fetal bovine serum. For spheroid cultures, cells were harvested, washed, and after centrifugation resuspended in DMEM supplemented with 2% (v/v) fetal bovine serum, 2 mM L-glutamine, 5 ng·mL⁻¹ epidermal growth factor, and 0.24% (w/v) methylcellulose (Sigma). Cells were pipetted onto the lid of a petri dish (12,500 cells/drop), the lid was inverted, and the hanging drops were cultured for 2 days (37 °C, 5% CO₂). The bottom of the petri dish was filled with 5 mL PBS for humidification. Subsequently, spheroids were harvested, seeded in 96-well Nunclon Sphera plates (Thermo Fisher), and challenged with the indicated substances. Irradiation of HNSCC cells was performed using an IBL 437C irradiator (CIS Bio International, Berlin, Germany) for 198 s (12 Gy) according to the manufacturer's instructions. Oxygen levels were modulated using a Whitley H35 Hypoxystation (Don Whitley Scientific, Shipley, UK). The following antibodies were used: ATF4 (#11815), ATF6 (#65880), BID (#2002), BIM (#2933), BAX (#5023), BAK (#12105), BCL-2 (#2872), BCL-W (#2724) BCL-XL (#2764), p53 (#4866): Cell Signaling (Beverly, MA, USA); MCL-1 (ab32087): abcam (Cambridge, UK); tubulin (#MS-581): Dunnlab (Asbach, Germany); and NOXA (114C307, #sc-56169): Santa Cruz (Santa Cruz, CA, USA). The following chemicals were used: MTT (3-[4,5-dimethylthiazol-2-yl]-2,5-diphenyl tetrazolium bromide), BAPTA-AM: Biomol, (Hamburg, Germany); ABT-737, WEHI-539, QVD-OPH: Hycultec (Beutelsbach, Germany); and ryanodine and cyclosporine A: Santa Cruz; SBFI and Fura-2: Thermo Fisher.

MTT-based cell viability assay

Cell viability was measured using MTT-based assays and has also been described in earlier studies [56,57]. Cells were seeded in 96-well plates (2 × 10⁴ cells/well) and challenged with the indicated concentrations of the indicated substances in duplicates (technical replicates). NaCl was added simultaneously. Unless indicated otherwise, cell viability was determined 18 h after stimulation using MTT staining (2 h at 37 °C). Staining intensity was measured at 595 nm, and the mean was calculated from the technical replicates of each experiment. The mean value of untreated controls was set to 100%. For any other condition, the MTT staining intensity is given relative to the corresponding untreated group (percentage of control). Data points shown are mean values (calculated from two technical replicates) of independent experiments ($n \geq 3$).

Western blot analysis

Western blot analysis was essentially performed as described previously [54].

siRNA experiments

siRNA oligonucleotides targeting BAX (#L-003308), NOXA (#L-005275), BIM (#L004383), MCL-1 (#L-004501-00-005), BCL-XL (#L-003458), p53 (#L-003329), and nontargeting control siRNA (#D-001810-10-05) were purchased from Dharmacon (Lafayette, CO, USA). PCI-1 and PCI-68 cells were transfected with 100 nM (BAX, NOXA, MCL-1, BCL-XL, p53, nontargeting control) and 200 nM (BIM) siRNA using DharmaFECT 1 transfection reagent (#T-2001-02) according to the manufacturer's instructions.

Quantitative PCR

Two micrograms of total RNA was transcribed into complementary DNA using the high-capacity cDNA reverse transcription kit (Applied Biosystems, Carlsbad, CA, USA). TaqMan gene expression assays were as follows: *BCL2L1* (encoding BCL-XL): Hs00236329_m1; *MCL1*: Hs01050896_m1; and *PMAIP1* (encoding NOXA): Hs00560402_m1 (Applied Biosystems). All assays were run on an ABI Prism 7900 sequence detector (Applied Biosystems). qRT-PCR reactions were performed in quadruplicates for each sample and normalized to the expression of

the housekeeping gene *HPRT1* (Hs02800695_m1). SDS 2.1 software (Applied Biosystems) calculated the mRNA levels.

Caspase activity assays

Fluorescence-based assessment of caspase activity has also been described in our previous studies [56,57]. Activity of caspase-3 and caspase-7 was measured using the caspase-3/-7 activity kit (AAT Bioquest, Sunnyvale, CA, USA) according to the manufacturer's instructions. A Victor 3 Multilabel Reader (PerkinElmer, Waltham, MA, USA) quantified emitted fluorescence.

Flow cytometry

Cell death was assessed by annexin-V and 7-AAD staining and has already been described in our earlier studies [56,57]. In brief, cells were challenged with the indicated concentrations of WEHI-539 in the presence and absence of NaCl for 8 h. Afterward, cells were stained with 7-AAD and annexin-V (4 °C for 15 min in the dark) following the standard procedures and analyzed immediately using a FACSCanto flow cytometer (BD Biosciences, Heidelberg, Germany) [58].

Measurement of intracellular Na⁺ and Ca²⁺ concentrations

Cells were seeded on FluoroDish Plates (#FD3510-100; World Precision Instruments, Sarasota, FL, USA). For Na⁺ measurements, cells were loaded with 10 μM SBFI (#S1264; Thermo Fisher) for 90 min at 37 °C. For Ca²⁺ measurements, cells were loaded with 2 μM Fura-2 (#F1221; Thermo Fisher) for 15 min at room temperature. Staining was performed in calcium-containing Tyrode's solution (140 mM NaCl, 4 mM KCl, 1 mM MgCl₂, 5 mM HEPES, 1 mM CaCl₂, 10 mM glucose) or calcium-free Tyrode's solution (140 mM NaCl, 4 mM KCl, 2 mM MgCl₂, 5 mM HEPES, 1 mM CaCl₂, 10 mM glucose). After washing with Tyrode's solution, cells were mounted on the stage of an inverted epifluorescence microscope (IonOptix Cooperation, Westwood, MA, USA). SBFI and Fura-2 were alternately excited at 340 and 380 nm. Emitted fluorescence was passed through a 515-nm long-pass filter, and acquisition with a photomultiplier was performed every 30 s for a duration of 10 min and analyzed using the IonWizard software (IonOptix Cooperation). After background subtraction, fluorescence intensities were normalized to F340/F380 at *t* = 0 min.

Wound healing assay

PCI-1 and PCI-68 cells were seeded in 6-well plates (2 × 10⁵ cells/well) and cultured to 90–100% confluence. The monolayer was 'scratched' with a 100 μL pipet tip and

carefully washed with PBS. Subsequently, cells were challenged with the indicated concentrations of NaCl and WEHI-539. Pictures were taken after 0, 24, and 48 h of incubation.

Calculation of combination index

Calculation of CI has also been described in our previous study [56]. Briefly, CI values were calculated with the freely available software COMPUSYN version 1.0 (ComboSyn Inc., Paramus, NJ, USA) using the median effect/combination index isobologram method [59]. In this model, CI values < 1 are considered synergistic and CI > 1 indicate antagonistic effects. Strength of synergism can be further graded: < 0.1, very strong synergism; 0.1–0.3, strong synergism; 0.3–0.7, synergism; 0.7–0.85, moderate synergism; 0.85–0.9, slight synergism; and 0.9–1.1, no synergism but nearly additive effects.

Acknowledgements

This work was supported by a fellowship from the Else-Kröner-Fresenius Stiftung awarded to SH. ME is supported by grants from the Universitätsstiftung Angela Schötz-Keilholz and the Universitätsstiftung Helga und Erwin Hartl. The sponsors had no role in study design, in the collection, analysis, and interpretation of data, in the writing of the report, and in the decision to submit the article for publication. Open access funding enabled and organized by Projekt DEAL.

Conflict of interest

The authors declare no conflict of interest.

Author contributions

ME, JJ, and SH designed the experiments. ME, SH, PN, and GK performed the experiments. RJB, SW, and KPH provided essential methodology. ME, SH, and GK analyzed the data. ME and SH wrote the paper.

References

- 1 Parkin DM, Bray F, Ferlay J & Pisani P (2005) Global cancer statistics, 2002. *CA Cancer J Clin* **55**, 74–108.
- 2 Alsahafi E, Begg K, Amelio I, Raulf N, Lucarelli P, Sauter T & Tavassoli M (2019) Clinical update on head and neck cancer: molecular biology and ongoing challenges. *Cell Death Dis* **10**, 540.
- 3 Bhola PD & Letai A (2016) Mitochondria-judges and executioners of cell death sentences. *Mol Cell* **61**, 695–704.

- 4 Green DR & Llamby F (2015) Cell death signaling. *Cold Spring Harb Perspect Biol* **7**, a006080.
- 5 Kale J, Osterlund EJ & Andrews DW (2018) BCL-2 family proteins: changing partners in the dance towards death. *Cell Death Differ* **25**, 65–80.
- 6 Ni Chonghaile T, Sarosiek KA, Vo TT, Ryan JA, Tammareddi A, Moore Vdel G, Deng J, Anderson KC, Richardson P, Tai YT *et al.* (2011) Pretreatment mitochondrial priming correlates with clinical response to cytotoxic chemotherapy. *Science* **334**, 1129–1133.
- 7 Montero J & Letai A (2018) Why do BCL-2 inhibitors work and where should we use them in the clinic? *Cell Death Differ* **25**, 56–64.
- 8 Kotschy A, Szlavik Z, Murray J, Davidson J, Maragno AL, Le Toumelin-Braizat G, Chanrion M, Kelly GL, Gong JN, Moujalled DM *et al.* (2016) The MCL1 inhibitor S63845 is tolerable and effective in diverse cancer models. *Nature* **538**, 477–482.
- 9 Souers AJ, Levenson JD, Boghaert ER, Ackler SL, Catron ND, Chen J, Dayton BD, Ding H, Enschede SH, Fairbrother WJ *et al.* (2013) ABT-199, a potent and selective BCL-2 inhibitor, achieves antitumor activity while sparing platelets. *Nat Med* **19**, 202–208.
- 10 Lessene G, Czabotar PE, Sleebs BE, Zobel K, Lowes KN, Adams JM, Baell JB, Colman PM, Deshayes K, Fairbrother WJ *et al.* (2013) Structure-guided design of a selective BCL-X(L) inhibitor. *Nat Chem Biol* **9**, 390–397.
- 11 Britt EL, Raman S, Leek K, Sheehy CH, Kim SW & Harada H (2019) Combination of fenretinide and ABT-263 induces apoptosis through NOXA for head and neck squamous cell carcinoma treatment. *PLoS One* **14**, e0219398.
- 12 Li R, Zang Y, Li C, Patel NS, Grandis JR & Johnson DE (2009) ABT-737 synergizes with chemotherapy to kill head and neck squamous cell carcinoma cells via a Noxa-mediated pathway. *Mol Pharmacol* **75**, 1231–1239.
- 13 Swiecicki PL, Bellile E, Sacco AG, Pearson AT, Taylor JM, Jackson TL, Chepeha DB, Spector ME, Shuman A, Malloy K *et al.* (2016) A phase II trial of the BCL-2 homolog domain 3 mimetic AT-101 in combination with docetaxel for recurrent, locally advanced, or metastatic head and neck cancer. *Invest New Drugs* **34**, 481–489.
- 14 Soderquist RS, Crawford L, Liu E, Lu M, Agarwal A, Anderson GR, Lin KH, Winter PS, Cakir M & Wood KC (2018) Systematic mapping of BCL-2 gene dependencies in cancer reveals molecular determinants of BH3 mimetic sensitivity. *Nat Commun* **9**, 3513.
- 15 Northcott JM, Dean IS, Mouw JK & Weaver VM (2018) Feeling stress: the mechanics of cancer progression and aggression. *Front Cell Dev Biol* **6**, 17.
- 16 Siegelin MD (2012) Utilization of the cellular stress response to sensitize cancer cells to TRAIL-mediated apoptosis. *Expert Opin Ther Targets* **16**, 801–817.
- 17 Singleton JR, Dixit VM & Feldman EL (1996) Type I insulin-like growth factor receptor activation regulates apoptotic proteins. *J Biol Chem* **271**, 31791–31794.
- 18 Alfieri RR & Petronini PG (2007) Hyperosmotic stress response: comparison with other cellular stresses. *Pflugers Arch* **454**, 173–185.
- 19 Burg MB, Ferraris JD & Dmitrieva NI (2007) Cellular response to hyperosmotic stresses. *Physiol Rev* **87**, 1441–1474.
- 20 Criollo A, Galluzzi L, Maiuri MC, Tasdemir E, Lavandro S & Kroemer G (2007) Mitochondrial control of cell death induced by hyperosmotic stress. *Apoptosis* **12**, 3–18.
- 21 Ow TJ, Fulcher CD, Thomas C, Broin PO, Lopez A, Reyna DE, Smith RV, Sarta C, Prystowsky MB, Schlecht NF *et al.* (2019) Optimal targeting of BCL-family proteins in head and neck squamous cell carcinoma requires inhibition of both BCL-xL and MCL-1. *Oncotarget* **10**, 494–510.
- 22 Crambert G, Hernandez T, Lamouroux C, Roth I, Dizin E, Martin PY, Feraille E & Hasler U (2014) Epithelial sodium channel abundance is decreased by an unfolded protein response induced by hyperosmolality. *Physiol Rep* **2**, e12169.
- 23 Cubillos-Ruiz JR, Bettigole SE & Glimcher LH (2017) Tumorigenic and immunosuppressive effects of endoplasmic reticulum stress in cancer. *Cell* **168**, 692–706.
- 24 Soderquist RS, Danilov AV & Eastman A (2014) Gossypol increases expression of the pro-apoptotic BH3-only protein NOXA through a novel mechanism involving phospholipase A2, cytoplasmic calcium, and endoplasmic reticulum stress. *J Biol Chem* **289**, 16190–16199.
- 25 Santulli G, Nakashima R, Yuan Q & Marks AR (2017) Intracellular calcium release channels: an update. *J Physiol* **595**, 3041–3051.
- 26 van Ginkel PR, Yan MB, Bhattacharya S, Polans AS & Kenealey JD (2015) Natural products induce a G protein-mediated calcium pathway activating p53 in cancer cells. *Toxicol Appl Pharmacol* **288**, 453–462.
- 27 Oda E, Ohki R, Murasawa H, Nemoto J, Shibue T, Yamashita T, Tokino T, Taniguchi T & Tanaka N (2000) Noxa, a BH3-only member of the Bcl-2 family and candidate mediator of p53-induced apoptosis. *Science* **288**, 1053–1058.
- 28 Laniado ME, Lalani EN, Fraser SP, Grimes JA, Bhangal G, Djamgoz MB & Abel PD (1997) Expression and functional analysis of voltage-activated Na⁺ channels in human prostate cancer cell lines and their contribution to invasion in vitro. *Am J Pathol* **150**, 1213–1221.
- 29 Fraser SP, Diss JK, Chioni AM, Mycielska ME, Pan H, Yamaci RF, Pani F, Siwy Z, Krasowska M, Grzywna Z *et al.* (2005) Voltage-gated sodium channel expression and potentiation of human breast cancer metastasis. *Clin Cancer Res* **11**, 5381–5389.

- 30 Roger S, Rollin J, Barascu A, Besson P, Raynal PI, Iochmann S, Lei M, Bougnoux P, Gruel Y & Le Guennec JY (2007) Voltage-gated sodium channels potentiate the invasive capacities of human non-small-cell lung cancer cell lines. *Int J Biochem Cell Biol* **39**, 774–786.
- 31 Bredell MG, Ernst J, El-Kochairi I, Dahlem Y, Ikenberg K & Schumann DM (2016) Current relevance of hypoxia in head and neck cancer. *Oncotarget* **7**, 50781–50804.
- 32 Qu Y, Dou B, Tan H, Feng Y, Wang N & Wang D (2019) Tumor microenvironment-driven non-cell-autonomous resistance to antineoplastic treatment. *Mol Cancer* **18**, 69.
- 33 Schmitz S & Machiels JP (2016) Targeting the tumor environment in squamous cell carcinoma of the head and neck. *Curr Treat Options Oncol* **17**, 37.
- 34 Chan N, Pires IM, Bencokova Z, Coackley C, Luoto KR, Bhogal N, Lakshman M, Gottipati P, Oliver FJ, Helleday T *et al.* (2010) Contextual synthetic lethality of cancer cell kill based on the tumor microenvironment. *Cancer Res* **70**, 8045–8054.
- 35 Nakajima W, Hicks MA, Tanaka N, Krystal GW & Harada H (2014) Noxa determines localization and stability of MCL-1 and consequently ABT-737 sensitivity in small cell lung cancer. *Cell Death Dis* **5**, e1052.
- 36 Liu Y, Mondello P, Erazo T, Tannan NB, Asgari Z, de Stanchina E, Nanjangud G, Seshan VE, Wang S, Wendel HG *et al.* (2018) NOXA genetic amplification or pharmacologic induction primes lymphoma cells to BCL2 inhibitor-induced cell death. *Proc Natl Acad Sci USA* **115**, 12034–12039.
- 37 Okumura K, Huang S & Sinicrope FA (2008) Induction of Noxa sensitizes human colorectal cancer cells expressing Mcl-1 to the small-molecule Bcl-2/Bcl-xL inhibitor, ABT-737. *Clin Cancer Res* **14**, 8132–8142.
- 38 Huang X, Yue W, Liu D, Yue J, Li J, Sun D, Yang M & Wang Z (2016) Monitoring the intracellular calcium response to a dynamic hypertonic environment. *Sci Rep* **6**, 23591.
- 39 Zhou Y, David MA, Chen X, Wan LQ, Duncan RL, Wang L & Lu XL (2016) Effects of osmolarity on the spontaneous calcium signaling of in situ juvenile and adult articular chondrocytes. *Ann Biomed Eng* **44**, 1138–1147.
- 40 Choi H, Chaiyamongkol W, Doolittle AC, Johnson ZI, Gogate SS, Schoepflin ZR, Shapiro IM & Risbud MV (2018) COX-2 expression mediated by calcium-TonEBP signaling axis under hyperosmotic conditions serves osmoprotective function in nucleus pulposus cells. *J Biol Chem* **293**, 8969–8981.
- 41 Chiong M, Parra V, Eisner V, Ibarra C, Maldonado C, Criollo A, Bravo R, Quiroga C, Contreras A, Vicencio JM *et al.* (2010) Parallel activation of Ca(2+)-induced survival and death pathways in cardiomyocytes by sorbitol-induced hyperosmotic stress. *Apoptosis* **15**, 887–903.
- 42 Dezaki K, Maeno E, Sato K, Akita T & Okada Y (2012) Early-phase occurrence of K⁺ and Cl⁻ efflux in addition to Ca²⁺ mobilization is a prerequisite to apoptosis in HeLa cells. *Apoptosis* **17**, 821–831.
- 43 Varghese E, Samuel SM, Sadiq Z, Kubatka P, Liskova A, Benacka J, Pazinka P, Kruzliak P & Busselberg D (2019) Anti-cancer agents in proliferation and cell death: the calcium connection. *Int J Mol Sci* **20**, 3017.
- 44 Stylianopoulos T, Martin JD, Snuderl M, Mpekris F, Jain SR & Jain RK (2013) Coevolution of solid stress and interstitial fluid pressure in tumors during progression: implications for vascular collapse. *Cancer Res* **73**, 3833–3841.
- 45 Kultz D & Chakravarty D (2001) Hyperosmolality in the form of elevated NaCl but not urea causes DNA damage in murine kidney cells. *Proc Natl Acad Sci USA* **98**, 1999–2004.
- 46 Yang T, Zhang A, Honegger M, Kohan DE, Mizel D, Sanders K, Hoidal JR, Briggs JP & Schnermann JB (2005) Hypertonic induction of COX-2 in collecting duct cells by reactive oxygen species of mitochondrial origin. *J Biol Chem* **280**, 34966–34973.
- 47 Di Ciano C, Nie Z, Szaszi K, Lewis A, Uruno T, Zhan X, Rotstein OD, Mak A & Kapus A (2002) Osmotic stress-induced remodeling of the cortical cytoskeleton. *Am J Physiol Cell Physiol* **283**, C850–C865.
- 48 Lang F, Busch GL, Ritter M, Volkl H, Waldegger S, Gulbins E & Haussinger D (1998) Functional significance of cell volume regulatory mechanisms. *Physiol Rev* **78**, 247–306.
- 49 Sheikh-Hamad D & Gustin MC (2004) MAP kinases and the adaptive response to hypertonicity: functional preservation from yeast to mammals. *Am J Physiol Renal Physiol* **287**, F1102–F1110.
- 50 Dmitrieva N, Kultz D, Michea L, Ferraris J & Burg M (2000) Protection of renal inner medullary epithelial cells from apoptosis by hypertonic stress-induced p53 activation. *J Biol Chem* **275**, 18243–18247.
- 51 Cohen DM, Wasserman JC & Gullans SR (1991) Immediate early gene and HSP70 expression in hyperosmotic stress in MDCK cells. *Am J Physiol* **261**, C594–C601.
- 52 Fritsch RM, Schneider G, Saur D, Scheibel M & Schmid RM (2007) Translational repression of MCL-1 couples stress-induced eIF2 alpha phosphorylation to mitochondrial apoptosis initiation. *J Biol Chem* **282**, 22551–22562.
- 53 Franco DL, Nojek IM, Molinero L, Coso OA & Costas MA (2002) Osmotic stress sensitizes naturally resistant cells to TNF-alpha-induced apoptosis. *Cell Death Differ* **9**, 1090–1098.
- 54 Sirtl S, Knoll G, Trinh DT, Lang I, Siegmund D, Gross S, Schuler-Thurner B, Neubert P, Jantsch J,

- Wajant H *et al.* (2018) Hypertonicity-enforced BCL-2 addiction unleashes the cytotoxic potential of death receptors. *Oncogene* **37**, 4122–4136.
- 55 Heo DS, Snyderman C, Gollin SM, Pan S, Walker E, Deka R, Barnes EL, Johnson JT, Herberman RB & Whiteside TL (1989) Biology, cytogenetics, and sensitivity to immunological effector cells of new head and neck squamous cell carcinoma lines. *Cancer Res* **49**, 5167–5175.
- 56 Heimer S, Knoll G, Steixner C, Calance DN, Trinh DT & Ehrenschrwender M (2018) Hypertonicity-imposed BCL-XL addiction primes colorectal cancer cells for death. *Cancer Lett* **435**, 23–31.
- 57 Heimer S, Knoll G, Schulze-Osthoff K & Ehrenschrwender M (2019) Raptinal bypasses BAX, BAK, and BOK for mitochondrial outer membrane permeabilization and intrinsic apoptosis. *Cell Death Dis* **10**, 556.
- 58 Telford W, Tamul K & Bradford J (2016) Measurement and characterization of apoptosis by flow cytometry. *Curr Protoc Cytom* **77**, 9.49.1–9.49.28.
- 59 Chou TC (2006) Theoretical basis, experimental design, and computerized simulation of synergism and antagonism in drug combination studies. *Pharmacol Rev* **58**, 621–681.